

# Probing Higgs in Type III Seesaw at the LHC

Priyotosh Bandyopadhyay<sup>a,c</sup>, Suyong Choi<sup>b</sup>, and Eung Jin Chun<sup>a</sup>, Kyungnam Min<sup>b</sup>

<sup>a</sup>*Korea Institute for Advanced Study, Seoul 130-722, Korea*

<sup>b</sup>*Department of Physics,*

*Korea University, Seoul 136-713, Korea*

<sup>c</sup>*Department of Physics and Helsinki Institute of Physics,  
University of Helsinki, FIN-00014, Finland*

## Abstract

We show that the type III seesaw mechanism opens up a promising possibility of searching the Higgs boson in the  $b\bar{b}$  channel through the Higgs production associated with a charged lepton coming from the decay of the triplet seesaw particle. In particular we look for the  $2b$  signals with trileptons or same-sign dileptons to construct the Higgs and the triplet fermion mass and calculate the reach with the integrated luminosity of  $10 \text{ fb}^{-1}$  at the 14 TeV LHC.

Finding the Higgs boson and thus verifying the electroweak symmetry breaking mechanism is a primary goal of the LHC. The recent LHC data constrain the Higgs mass in a narrow range of 115–130 GeV [1]. For such a low mass Higgs boson, its discovery relies on the combination of several channels based on the gluon fusion production, in particular,  $gg \rightarrow h \rightarrow \gamma\gamma$ . Another interesting channel is the associated Higgs boson production  $p\bar{p} \rightarrow W(Z)h$  followed by the dominant Higgs decay  $h \rightarrow b\bar{b}$  and leptonic decays of  $W(Z)$  for which a low significance due to large backgrounds can be overcome by using subjet techniques in a boosted regime [2]. Probing such a channel is important as it can provide an independent information on the Higgs boson coupling to gauge bosons and  $b$  quarks.

The purpose of this work is to explore another possibility for the Higgs discovery which arises in the type III seesaw mechanism, where the origin of the observed neutrino masses and mixing is attributed to  $SU(2)$  triplet fermions with hypercharge zero [3]. Such new particles can be produced through the electroweak interaction and subsequently decay to a lepton plus  $W$ ,  $Z$  or  $h$ . These signatures can be traced successfully to reconstruct the new triplets and thus confirm the type III seesaw mechanism [4–8]. Among these type III seesaw signatures, we focus on the Higgs production associated with a charged lepton followed by the Higgs decay  $h \rightarrow b\bar{b}$  to show that this channel provides a promising search channel for the low mass Higgs boson.

The type III seesaw mechanism introduces  $SU(2)_L$  triplet fermions with  $Y = 0$ ,  $\Sigma = (\Sigma^+, \Sigma^0, \Sigma^-)$ , which can be written in a matrix form:

$$\Sigma = \begin{pmatrix} \Sigma^0 & \sqrt{2}\Sigma^+ \\ \sqrt{2}\Sigma^- & -\Sigma^0 \end{pmatrix}. \quad (1)$$

Then the gauge invariant Yukawa terms are

$$\mathcal{L} = [y_i H \bar{\varepsilon} \Sigma P_L l_i + h.c.] + \frac{1}{4} m_\Sigma \text{Tr} [\bar{\Sigma} \Sigma] \quad (2)$$

where  $l_i$  is the lepton doublet and  $H$  is the Higgs doublet:  $l_i = (\nu_i, e_i)_L$  and  $H = (H^+, H^0)$ . In the unitary gauge,

$H^+ = 0$  and  $H^0 = v + h/\sqrt{2}$  with  $v = 174 \text{ GeV}$ , we get

$$\mathcal{L}_{Yukawa} = y_i \left[ \sqrt{2} \bar{\Sigma}^- P_L e_i + \bar{\Sigma}^0 P_L \nu_i + h.c. \right] \frac{h}{\sqrt{2}}. \quad (3)$$

Here we take only one generation of the triplet for our illustration. Note that the neutrinos get a seesaw mass  $m_{ij}^\nu = y_i y_j v^2 / m_\Sigma$  which becomes of the order 0.1 eV for  $y_i \sim 10^{-6}$  and  $m_\Sigma \sim 1 \text{ TeV}$ . The neutrino Dirac mass,  $y_i v$ , induces mixing between  $l$  and  $\Sigma$ . The mixing angles for the neutral and charged part are

$$\theta_{\nu_i} \approx \frac{y_i v}{m_\Sigma} \quad \text{and} \quad \theta_{l_i} \approx \sqrt{2} \frac{y_i v}{m_\Sigma} \quad (4)$$

respectively. Due to the  $l$ – $\Sigma$  mixing (4), we get the mixed gauge interaction as follows;

$$\begin{aligned} \mathcal{L}_{gauge} = & -g\theta_{\nu_i} W_\mu^+ \left[ \frac{1}{\sqrt{2}} \bar{\Sigma}^0 \gamma^\mu P_L e_i + \bar{\nu}_i \gamma^\mu R_R \Sigma^- \right] \\ & -g\theta_{\nu_i} W_\mu^- \left[ \frac{1}{\sqrt{2}} \bar{e}_i \gamma^\mu P_L \Sigma^0 + \bar{\Sigma}^- \gamma^\mu P_R \nu_i \right] \\ & + \frac{g\theta_{\nu_i}}{2c_W} Z_\mu \left[ \sqrt{2} \bar{\Sigma}^- \gamma^\mu P_L e_i + \sqrt{2} \bar{e}_i \gamma^\mu P_L \Sigma^- - \bar{\Sigma}^0 \gamma^\mu \gamma_5 \nu_i \right]. \end{aligned} \quad (5)$$

Thus, the electroweak production of the triplets at the LHC,  $p\bar{p} \rightarrow \Sigma^\pm \Sigma^0, \Sigma^\pm \Sigma^\mp$ , will leave bunch of multi-lepton final states followed by the triplet decays:

$$\begin{aligned} \Sigma^\pm & \rightarrow l^\pm h, \quad l^\pm Z^0, \quad \nu W^\pm, \quad \Sigma^0 \pi^\pm \\ \Sigma^0 & \rightarrow \nu h, \quad \nu Z^0, \quad l^\pm W^\mp. \end{aligned} \quad (6)$$

Among them, trilepton ( $3l$ ) and same sign dilepton (SSD) signals were shown to provide the most promising channels for the triplet search [5]. This is also true for probing the Higgs boson in the type III seesaw. That is, the main channels for the Higgs search studied in this paper will be  $3l$  and SSD final states coming from  $\Sigma^\pm \Sigma^0$  as follows:

$$l^\pm h l W(l\nu), \quad l^\pm h \nu Z(ll), \quad l^\pm Z(ll) \nu h; \quad l^\pm h l^\pm W^\mp(l\nu, jj).$$

For the collider analysis, we have chosen two benchmark points, BP1 and BP2, with  $m_\Sigma = 250$  and  $400 \text{ GeV}$ ,

Production cross-sections (fb)		
$m_\Sigma$	250 GeV	400 GeV
$\Sigma^+\Sigma^0$	439.1	73.8
$\Sigma^+\Sigma^-$	320.0	50.0
$\Sigma^-\Sigma^0$	221.8	32.3

TABLE I: Two benchmark production cross-sections.

Decay modes	Branching ratios	
$m_\Sigma$	250 GeV	400 GeV
$\Sigma^0 \rightarrow h\nu$	0.17	0.22
$\Sigma^0 \rightarrow Z\nu$	0.27	0.26
$\Sigma^0 \rightarrow W^\pm l^\mp$	0.56	0.52
$\Sigma^\pm \rightarrow h l^\pm$	0.17	0.22
$\Sigma^\pm \rightarrow Z l^\pm$	0.27	0.26
$\Sigma^\pm \rightarrow W^\pm \nu$	0.55	0.52
$\Sigma^\pm \rightarrow \Sigma^0 \pi^\pm$	0.009	0.003

TABLE II: Triplet branching ratios for  $\tilde{m}_\nu = 10$  meV.

respectively, taking the Higgs mass of 120 GeV. The production cross-sections of the triplet pairs at the 14 TeV LHC corresponding to BP1 and BP2 are listed in Table I. The branching ratios of the triplet decay are calculated in Table II. The decay rate of  $\Sigma^\pm \rightarrow \Sigma^0 \pi^\pm$  is suppressed by a small mass splitting between  $\Sigma^\pm$  and  $\Sigma^0$  arising from one-loop correction, while the other decay rates are proportional to  $y_i^2$  coming from the mixing (4) [4]. The size of the neutrino Yukawa coupling  $y$  can be quantified by the effective neutrino mass  $\tilde{m}_\nu \equiv |y|^2 v^2 / m_\Sigma$  where we take, in our analysis,  $y = y_1$  or  $y_2$  denoting the electron or muon neutrino Yukawa coupling, respectively. When  $\tilde{m}_\nu$  is sufficiently small, the triplet decays will occur at large displaced vertices and thus enable us to trace a displaced Higgs production free from backgrounds [9]. In this work, we do not look for the signatures with displaced vertices as our analysis can be applied to any value of  $\tilde{m}_\nu$ . For our presentation, we set  $\tilde{m}_\nu = 10$  meV corresponding to the solar neutrino mass scale.

In this study, **MadGraph** [10] has been used for generating parton-level events for the relevant processes. The LHEF interface [11] was then used to pass the **MadGraph**-generated events to **PYTHIA** [12]. We use **CTEQ6L** parton distribution function (PDF) [13, 14]. In **MadGraph** we opted for the lowest order  $\alpha_s$  evaluation, which is appropriate for a lowest order PDF like **CTEQ6L**. The renormalization/factorization scale in **MadGraph** is set at  $\sqrt{s}$ . This choice of scale results in a somewhat conservative estimate for the event rates. ISR/FSR were switched on in **PYTHIA** for a realistic simulation. For this analysis we have assumed a  $b$ -jet tagging efficiency of  $\geq 50\%$  [15]. For hadronic level simulation we have used **PYCELL**, the toy calorimeter simulation provided in **PYTHIA**, with the following criteria:

- the calorimeter coverage is  $|\eta| < 4.5$  and the seg-

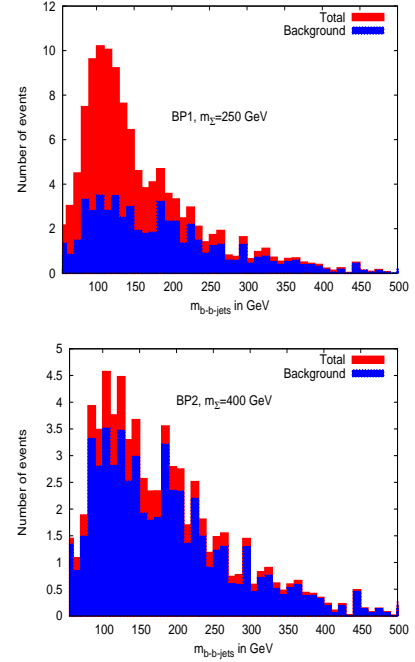


FIG. 1: The  $b$ - $b$  invariant mass from  $\geq 2b + 3l$  final states.

$2b + 3l$							
Signal		Backgrounds					
BP1	BP2	$t\bar{t}$	$t\bar{t}b\bar{b}$	$t\bar{t}Z$	$t\bar{t}h$	$VV$	$t\bar{t}W$
116.89	40.32	5.0	1.77	31.53	9.86	0.0	8.67

$m_{b-b}$							
Signal		Backgrounds					
BP1	BP2	$t\bar{t}$	$t\bar{t}b\bar{b}$	$t\bar{t}Z$	$t\bar{t}h$	$VV$	$t\bar{t}W$
28.44	4.46	1.0	0.50	8.3	2.2	0.0	2.5

$m_{b-b-l}$							
Signal		Backgrounds					
		$t\bar{t}$	$t\bar{t}b\bar{b}$	$t\bar{t}Z$	$t\bar{t}h$	$VV$	$t\bar{t}W$
BP1	61.89	2.0	0.1	5.9	1.5	0.0	0.9
BP2	5.19	0.0	0.0	1.5	0.06	0.0	0.5

TABLE III: Number of events for  $2b + 3l$ ; for  $m_{b-b}$  within  $120 \pm 25$  GeV; and for  $m_{b-b-l}$  within  $250$  ( $400$ )  $\pm 50$  GeV.

mentation is given by  $\Delta\eta \times \Delta\phi = 0.09 \times 0.09$  which resembles a generic LHC detector;

- a cone algorithm with  $\Delta R = \sqrt{\Delta\eta^2 + \Delta\phi^2} = 0.5$  has been used for jet finding;
- $p_{T,min}^{jet} = 20$  GeV and jets are ordered in  $p_T$ ;
- leptons ( $\ell = e, \mu$ ) are selected with  $p_T \geq 20$  GeV and  $|\eta| \leq 2.5$ ;
- no jet should match with a hard lepton in the event.

**Higgs search with  $2b + 3l$ :** For the Higgs event selection, we first study the final state topology with at

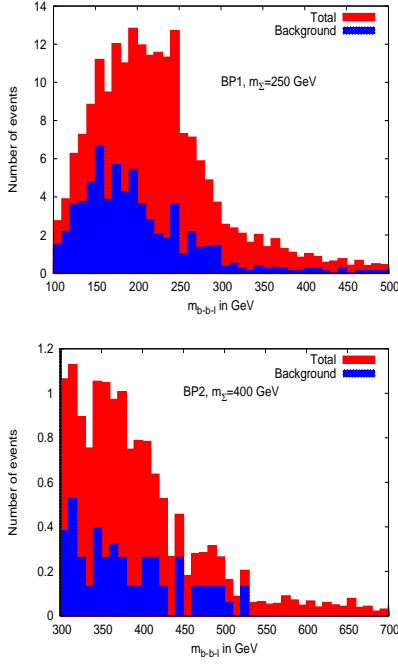


FIG. 2: The  $b-b-l$  invariant mass from  $\geq 2b + 3l$  final states.

least two tagged  $b$ -jets and at least three isolated leptons. Dominant Standard Model (SM) backgrounds are denoted in Table III. Here  $VV + n$  - jets do not contribute as potential backgrounds. The number of the signal and background events for the two benchmark points are listed in Table III for an integrated luminosity of  $10 \text{ fb}^{-1}$  at the 14 TeV LHC. As we can see from the Table III the significance for BP1 is  $\sim 9\sigma$  and that of BP2 is  $4\sigma$  at  $10 \text{ fb}^{-1}$  of integrated luminosity.

The  $b$ -jet pair invariant mass distribution, after the event selection, is presented in Figure 1 which shows the smeared distribution for lower invariant mass due to the  $Z$  peak contribution. Thus reconstructing Higgs mass does not increase the signal significance. Selecting events within the window of  $95 \text{ GeV} \leq m_{b-b} \leq 145 \text{ GeV}$  as in Table III, we get the required luminosity for for  $5\sigma$  signal significance  $13.3 \text{ fb}^{-1}$  for BP1 and  $238 \text{ fb}^{-1}$  for BP2.

To check if the reconstructed Higgses are indeed from the triplet decay, invariant mass distribution of the two  $b$ -jets with one of the lepton among the tree isolated leptons is constructed. In principle among the three leptons the right one will peak at the triplet mass and the others will contribute in the combinatorial background. For this, we select the  $b$ -jets within 60-150 GeV of the invariant mass distribution. Figure 2 describes the invariant of distribution of  $b-b-l$ . We then select for  $200 \text{ GeV} \leq m_{b-b-l} \leq 300 \text{ GeV}$  for BP1,  $350 \text{ GeV} \leq m_{b-b-l} \leq 450 \text{ GeV}$  for BP2. From the Figure 2 we can see that the distribution has a edge at the triplet mass. This is because, one low  $p_T$  lepton, coming from the decay of gauge boson, contributes in the lower end of the mass spectrum. This makes the peak asym-

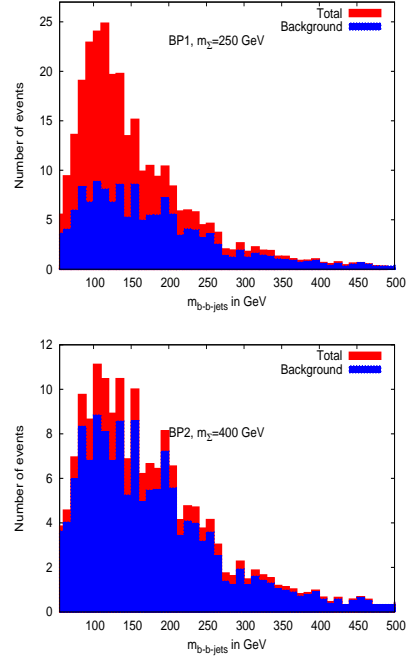


FIG. 3: The  $b-b$  invariant mass from  $\geq 2b + \text{SSD}$  final states.

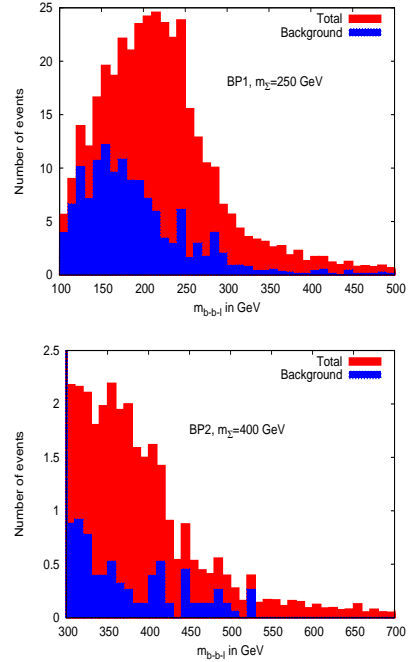


FIG. 4: The  $b-b-l$  invariant mass from  $\geq 2b + \text{SSD}$  final states.

metric in nature. From the signal numbers listed in Table III, one finds the significances of  $\sim 7.3\sigma$  for BP1 and  $\sim 2\sigma$  for BP2.

**Higgs search with  $2b + \text{SSD}$ :** The final states with same-sign dileptons are also free from severe Standard Model backgrounds. The final decay modes from  $\Sigma$  that contribute to the process are  $hlWl$ ,  $hlZl$ ,  $ZlZl$ ,  $ZlWl$

$\geq 2b - \text{jet} + \text{SSD}$							
Signal		Backgrounds					
BP1	BP2	$t\bar{t}$	$t\bar{t}b\bar{b}$	$t\bar{t}Z$	$t\bar{t}h$	$VV$	$t\bar{t}W$
127.38	29.09	24.0	7.5	41.6	29.0	0.0	41.4

$m_{b-b}$							
Signal		Backgrounds					
BP1	BP2	$t\bar{t}$	$t\bar{t}b\bar{b}$	$t\bar{t}Z$	$t\bar{t}h$	$VV$	$t\bar{t}W$
60.61	10.39	8.0	3.0	10.6	6.5	0.0	9.6

$m_{b-b-l}$							
Signal		Backgrounds					
		$t\bar{t}$	$t\bar{t}b\bar{b}$	$t\bar{t}Z$	$t\bar{t}h$	$VV$	$t\bar{t}W$
BP1	117.37	4.0	0.35	7.00	2.67	0.0	2.50
BP2	11.74	0.0	0.0	1.71	0.12	0.0	1.05

TABLE IV: Number of events for  $2b + \text{SSD}$ ; for  $m_{b-b}$  within  $120 \pm 25$  GeV; and for  $m_{b-b-l}$  within  $250$  ( $400$ )  $\pm 50$  GeV.

respectively. Basically, the  $3l$  events always carry same sign dileptons and will contribute to this final state. In addition, signal acceptance is gained by requiring two or more leptons. If one of the leptons in a tripleton event does not pass the acceptance, there is a chance that it will still be accepted in the SSD selection.

We select the events with at least two  $b$ -tagged jets and at least two isolated same-sign leptons in the final states. In Table IV we present the corresponding signal numbers for the two benchmark points and the SM backgrounds at  $10 \text{ fb}^{-1}$  of integrated luminosity. The signal significances are  $\sim 8\sigma$  for BP1, and  $2.2\sigma$  for BP2.

After analyzing the final state with SSD and  $2b$ -jets we construct the Higgs mass peak. We plot the invariant mass distribution of these to  $b$ -jets which peak around the  $Z$  and Higgs mass in Figure 3. Selecting events  $95\text{GeV} \leq$

$m_{b-b} \leq 145\text{GeV}$  we get the signal numbers for the Higgs mass peak as listed in Table IV. The corresponding signal significance over SM backgrounds are  $6.11\sigma$ , and  $1.5\sigma$  for BP1, and BP2, respectively. This shows the SSD events are better than the  $3l$  events in probing the Higgs boson.

Similar to the  $3l$  case, we reconstruct the triplet mass from the selected Higgs events and the leptons in the final state. For that we take again the  $b$ -jets within the mass window of 60-150 GeV and plot the invariant mass distribution with the lepton in the final state in Figure 4. Selecting the events within the windows of  $200\text{GeV} \leq m_{b-b-l} \leq 300\text{GeV}$  for BP1, and  $350\text{GeV} \leq m_{b-b-l} \leq 450\text{GeV}$  for BP2, we get the result in Table IV. In this case the significance really gets enhanced;  $\simeq 10\sigma$  for BP1, and  $3\sigma$  for BP2.

In conclusion, we examined  $b$ -jet pair signals from Higgs in association with tripletons or same-sign dileptons in the type III seesaw mechanism. These channels enough significances over the Standard Model backgrounds, in particular, in the high  $p_T$  regime, and thus provide viable channels for the light Higgs boson search. Early data of the 14 TeV LHC will enable us to reconstruct the Higgs boson coming from the triplet decay through  $b-b$  and  $b-b-l$  invariant mass distributions for relatively lower triplet mass. On the other hand the reach goes down rapidly for higher triplet mass due to the strong depletion of the triplet production cross-section which will be overcome by further accumulation of the luminosity.

**Acknowledgments:** EJC was supported by Korea Neutrino Research Center through National Research Foundation Grant (2009-0083526). SC was supported by National Research Foundation Grant (2009-0069251). We also acknowledge Roberto Francheschini for providing us with the MadGraph model files implementing the Type III seesaw model.

- 
- [1] ATLAS Collaboration, ATLAS-CONF-2011-163; CMS Collaboration, CMS-PAS-HIG-11-032.
  - [2] J. M. Butterworth, A. R. Davison, M. Rubin and G. P. Salam, Phys. Rev. Lett. **100**, 242001 (2008) [arXiv:0802.2470 [hep-ph]].
  - [3] R. Foot, H. Lew, X. G. He and G. C. Joshi, Z. Phys. C **44** (1989) 441.
  - [4] R. Franceschini, T. Hambye and A. Strumia, Phys. Rev. D **78** (2008) 033002 [arXiv:0805.1613 [hep-ph]].
  - [5] F. del Aguila and J. A. Aguilar-Saavedra, Nucl. Phys. B **813** (2009) 22 [arXiv:0808.2468 [hep-ph]].
  - [6] A. Arhrib *et al.*, [arXiv:0904.2390 [hep-ph]].
  - [7] P. Bandyopadhyay, S. Choubey and M. Mitra, JHEP **0910** (2009) 012 [arXiv:0906.5330 [hep-ph]].
  - [8] T. Li and X. G. He, Phys. Rev. D **80** (2009) 093003 [arXiv:0907.4193 [hep-ph]].
  - [9] P. Bandyopadhyay and E. J. Chun, JHEP **1011**, 006 (2010) [arXiv:1007.2281 [hep-ph]].
  - [10] J. Alwall *et al.*, JHEP **0709**, 028 (2007) [arXiv:0706.2334 [hep-ph]].
  - [11] J. Alwall *et al.*, Comput. Phys. Commun. **176**, 300 (2007) [arXiv:hep-ph/0609017].
  - [12] T. Sjostrand, L. Lonnblad and S. Mrenna, [arXiv:hep-ph/0108264].
  - [13] H. L. Lai *et al.* [CTEQ Collaboration], Eur. Phys. J. C **12**, 375 (2000) [arXiv:hep-ph/9903282].
  - [14] J. Pumplin *et al.*, JHEP **0207**, 012 (2002) [arXiv:hep-ph/0201195].
  - [15] H. Baer *et al.*, Phys. Rev. D **75**, 095010 (2007) [arXiv:hep-ph/0703289].